Article

Preparation and Characterization of Paper Mill Sludge-based Co/Fe Composite Catalyst and the Influence of Various Inorganic Anions During the Fenton-like oxidation Process

Xiaoyang Chen [*] , Jiahua Yu , Min Xiao , Ailan Yan , and Yiyan Lv [*]

Article

Preparation and Characterization of Paper Mill Sludge-Based Co/Fe Composite Catalyst and the Influence of Various Inorganic Anions During the Fenton-Like Oxidation Process

Xiaoyang Chen [1],*, Jiahua Yu [1,2], Min Xiao [3], Ailan Yan [1] and Yiyan Lv [4],*

[1] College of Environmental Science and Engineering, Zhejiang University of Water Resources and Electric Power, Hangzhou 310018, China

[2] School of Petrochemical Engineering & Environment, Zhejiang Ocean University, Zhoushan 316022, China

[3] Key Laboratory of Regional Environment and Eco-Remediation (Ministry of Education), Shenyang University, Shenyang 110044, China

[4] Zhejiang Huadong Geotechnical Investigation & Design Institute Co, Ltd, Hangzhou 310030, China

* Correspondence: chenxy@zjweu.edu.cn (X.C.); lv_yy3@hdec.com (Y.L.); Tel.: +86-0571-86929386

Abstract: Sewage sludge, particularly paper mill sludge, is carbonaceous by nature. It can be employed as a heterogeneous catalyst for Fenton-like reactions to attain high catalytic activity and long-term stability. In this paper, the Co/Fe bimetallic composite catalyst was prepared by taking paper mill sludge as the carrier via impregnation and calcination. This catalyst was employed to catalyze peroxymonosulfate (PMS), to produce $SO_4^{\bullet-}$, which has strong oxidizing power. This study focused on determining the optimal preparation conditions, characterization of the catalyst, and investigating the effects of various inorganic anions on the degradation of Rhodamine B (RhB) in the Co/Fe-PMS system. The optimal catalyst preparation condition was found to be a 0.5 mol/L impregnation concentration, with the best ratio of $Co(NO_3)_2$ to $FeSO_4$ solution being 7:3. The presence of Co and Fe in the catalyst was determined through FTIR and XRD analyses. The catalyst is a porous material with magnetic properties and is capable of degrading more than 95% of RhB within two minutes. It was found that $H_2PO_4^-$, Cl^-, and HCO_3^- had negative impacts on the degradation of RhB. Low concentrations of NO_3^- had a positive effect, whereas high concentrations of NO_3^- had a negative effect. This study presents a novel method for preparing highly efficient Fenton-like catalysts and offers an effective approach for sludge utilization.

Keywords: Sewage sludge; Co/Fe catalyst; Sulfate radical; Rhodamine B (RhB); Inorganic ion

1. Introduction

In recent years, there has been a significant increase interest in the study of advanced oxidation technology (AOTs) that utilizes sulfate radicals ($SO_4^{\bullet-}$) for degrading organic pollutants [1–4]. The principle behind this process is the use of the highly oxidative nature of $SO_4^{\bullet-}$ to break down organic pollutants into non-toxic or low-toxic small molecules, or even to completely decompose them into CO_2, H_2O, and the corresponding inorganic ions, thereby achieving effective pollutant degradation [4,5]. Compared with the conventional Fenton reagent, which takes $\bullet OH$ as the main active species, $SO_4^{\bullet-}$ shows stronger oxidative properties and operates effectively within a broader pH range from 3 to 8, making it a more applicable [5–7]. There are two primary methods for generating $SO_4^{\bullet-}$: (1) by pyrolyzing peroxymonosulfate (PMS) under high temperature or radiation, and (2) through transition metal activation of PMS [7–10]. The conventional PMS-based AOTs are limited by challenges such as the short service life of catalysts and low efficiency of reactive oxygen species (ROS) utilization [10,11]. These issues stem from the agglomeration of nanocatalyst particles in traditional

heterogeneous catalytic systems, which hinder the rapid interaction between generated ROS and the pollutants [12]. Additionally, concerns related to catalyst recovery and potential secondary pollution from catalyst dissolution must be addressed [13,14]. Among these methods, the Co-catalyzed PMS route is the most widely used, while Co-catalyzed PMS faces inherent drawbacks, including the poor recyclability of Co^{2+} and the environmental risks associated with cobalt, which can lead to secondary pollution [15,16]. To address these shortcomings, immobilizing cobalt ions on suitable carriers for heterogeneous reactions emerges as a promising solution. The selection of structurally stable and cost-effective carriers is crucial in overcoming these challenges [17,18].

With the increasing volume of industrial wastewater treatment, there is a significant rise in the generation of sludge [19,20]. Traditional sludge treatment methods such as ocean dumping, landfill, and incineration, pose environmental risks to soil, water, and air [21,22]. Therefore, the development of non-polluting, high-value-added sludge treatment methods has become a critical issue [21–24]. In fact, sludge, especially from paper mills, contains a large amount of carbon, and can be converted into porous activated carbon after chemical treatment or other treatment conditions [25,26]. Sludge pyrolysis to produce activated carbon is an excellent treatment method, as it reduces the volume of sludge, destroys most pathogens and microorganisms, and immobilizes toxic metals [27–30]. Numerous studies have shown that mesoporous materials derived from sludge pyrolysis can serve as efficient and stable carriers for heterogeneous Fenton catalysts, offering high catalytic activity and long-term stability [31,32].

In this study, paper mill sludge was utilized as a carrier to prepare Co/Fe bimetallic composite catalysts, which were aimed at catalyzing the degradation of rhodamine B by PMS. The optimal preparation conditions for the Co/Fe bimetallic composite catalysts and the impact of various inorganic ions on the reaction system were studied. This approach not only addressed the immobilization of cobalt ions but also utilized sludge resourcefully to mitigate environmental pollution.

2. Materials and Methods

2.1. Reagents

The experimental paper sludge was sourced from Chunan Paper Mill, located in Fuyang District, Hangzhou City. It was initially dried at 105°C until a constant weight was achieved, then sieved through an 80-mesh filter and stored in sealed conditions to prevent contamination.

Oxone was obtained from Zhejiang Shangyu Jiehua Chemical Co. Methanol, Rhodamine B (RhB), $Co(NO_3)_2$, and $FeSO_4$ were all of analytical grade and purchased from Sinopharm Chemical Reagent Co. All solutions were prepared using Milli-Q pure water

2.2. Catalyst Preparation

A 10 g sample of dried paper sludge underwent impregnation with a specified concentration of $FeSO_4$ and $Co(NO_3)_2$ (30 mL) for 1 hour, followed by stirring for 24 hours. The resulting product was then dried at 105°C for 12 hours. This product was subjected to pyrolysis in a tube furnace for 2 hours, with a heating rate of 20°C/min and a nitrogen flow rate of 0.1 m^3/h. After pyrolysis, the product was ground and washed with ultrapure water until the conductivity of the wash water remained constant. Finally, the catalyst was dried at 80°C to a constant weight.

2.3. RhB degradation

All batch experiments were conducted in 250 mL conical flasks equipped with magnetic stirrers at room temperature. In each experiment, 0.05 g of catalyst was added to 150 mL of 50 mg/L Rhodamine B solution. The reaction mixture was stirred in the dark for 1 hour to allow for catalyst dispersion and adsorption-desorption equilibrium. After the first sampling, PMS was introduced to initiate the reaction. Samples were taken at specific time intervals, and the reaction was terminated by adding an equal volume of methanol immediately after sampling. The concentration of Rhodamine B was measured using a UV spectrophotometer (UV-3150, Shimadzu) at a wavelength of 554 nm.

2.4. Methods of analysis

The functional groups of the synthesized catalysts were analyzed using Fourier Transform Infrared Spectroscopy (FT-IR, Thermo Nicolet 380, USA). The crystal structure of the catalyst was characterized by X-ray Diffraction (XRD, Bruker D8 Advance, German). The specific surface area of the

catalyst was determined using the BET method (Conta noa2000e, USA). The surface morphology of the catalyst was examined by Scanning Electron Microscopy (SEM) with a Hitachi S-3400N (Japan).

3. Results

3.1. Study on the optimum preparation conditions of paper mill sludge-based Fe/Co composite catalysts

Figure 1 illustrates the effect of various impregnation concentrations during catalyst preparation. The results shows that the degradation rate of the RhB increases with the $Co(NO_3)_2$ concentration until it reaches 0.5 mol/L, at which point more than 95% of the RhB is degraded rapidly. Further increases in concentration do not significantly enhance the degradation rate. Initially, increasing the $Co(NO_3)_2$ concentration increases the number of active sites on the surface of the paper sludge, enhancing its catalytic properties. However, when the concentration is too low, achieving complete degradation of rhodamine B within a short time frame becomes impossible. As the concentration continues to rise, the amount of cobalt that the paper sludge can absorb reaches saturation, and further increases no longer contribute to additional cobalt loading. Beyond this point, any additional cobalt will not enhance catalytic performance and may leach from the sludge during post-calcination washing. Thus, the optimal impregnation concentration for the paper sludge-based Co catalyst is 0.5 mol/L.
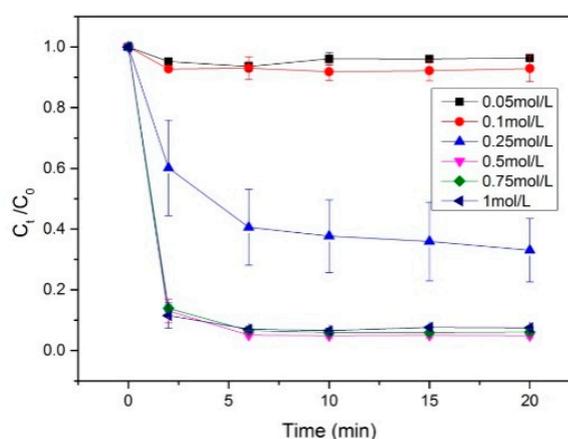

Figure 1. Effect of $Co(NO_3)_2$ concentration on RhB degradation during Co-PMS system.

([RhB]= 50mg/L, [PMS]=0.07mol/L, [catalysts]= 0.33g/L)

To explore the preparation of Co/Fe composite catalysts, the effects of various Co/Fe ratios on the degradation of rhodamine B were investigated (Figure 2). The results reveal that at a 10% Co proportion, the catalyst was unable to completely degrade rhodamine B, and the reaction proceeded slowly. However, as the Co proportion was incrementally increased, the RhB degradation rate also increased. At a 30% Co proportion, the dye RhB was completely degraded. When the Co proportion was further increased to 70%, the reaction completed within 2 minutes. Nonetheless, degradation efficiency was lower when exclusively using Cobalt catalyst, compared to a Co/Fe composite catalysts ratio of at least 7:3. This suggests that the catalytic performance is enhanced with bimetallic loading compared to single-metal catalysts.
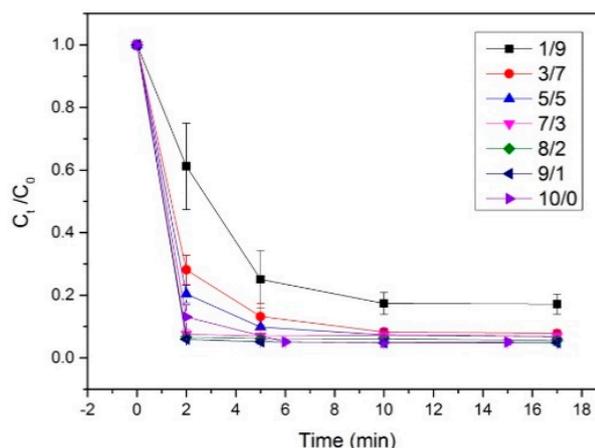
Figure 2. Effect of different Co/Fe ixture ratio in PMS-Co on RhB degradation.

([RhB]= 50mg/L, [PMS]=0.07mol/L, [catalysts]= 0.33g/L)

3.2. Characterization of paper mill sludge-based Co/Fe composite catalysts

The paper mill sludge-based Co/Fe composite catalysts were characterized by FTIR and XRD spectra analysis (Figure 3). The FTIR analysis (Figure 3a) reveals peaks at 3400 cm^{-1}, corresponding to O-H stretching vibrations, and at 875 cm^{-1}, characteristic of Si-O symmetric stretching vibrations [33]. Additional peaks at 675 cm^{-1} and 464 cm^{-1} are attributed to Si-O-Fe stretching and bending vibrations, respectively [33]. Peaks at 594 cm^{-1} and 667 cm^{-1} correspond to Co-O stretching and bending vibrations, respectively [34]. The presence of iron (Fe) and cobalt (Co) is essential to the catalytic process in this experiment. The spectral data indicate the presence of Si-O-Fe and Co-O bonds within the chemical structure of the catalysts, which contribute to their enhanced catalytic performance. Analysis of the XRD spectra (Figure 3b) reveals peaks at 2θ values of 26.83°, 39.49°, and 48.92°, corresponding to the (002), (200), and (113) crystal planes of Fe_2O_3 microcrystals, respectively. Additionally, peaks at 2θ values of 47.71° and 48.968° correspond to the (110) and (102) crystal planes of $FeSi_2$ microcrystals. Co_3O_4 microcrystals were identified at 2θ values of 36.34° and 43° [34]. These results indicate that after calcination, the oxides of Fe and Co, specifically Fe_2O_3 and Co_3O_4, are present on the catalyst surface. Moreover, the presence of $FeSi_2$ suggests that iron is chemically bonded to the paper sludge, which serves as a carrier. This bonding enhances the stability of the catalyst.
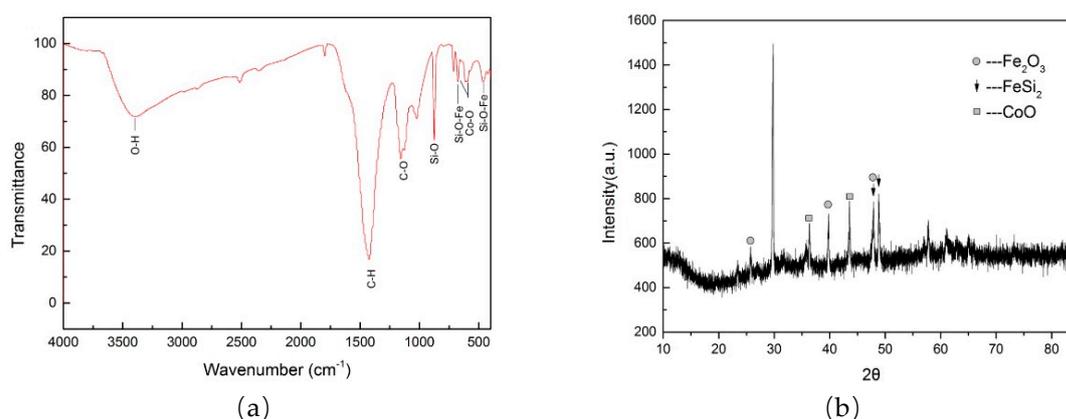

(a)

(b)

Figure 3. The FTIR (a) and XRD (b) spectra of the Co/Fe composite catalysts.

The Raman spectrum of the paper mill sludge-based Co/Fe composite catalyst is shown in Figure 4(a). The spectrum features two prominent diffraction peaks at 1320 cm^{-1} and 1570 cm^{-1}, labeled as the D and G peaks, respectively. The D peak is associated with the sp^3 hybridization of carbon atoms, indicating defects or distortions within the crystalline lattice. Conversely, the G peak corresponds to the sp^2 hybridization of carbon atoms, which is induced by the active vibration of the E_{2g} mode [35]. These peaks indicate the presence of carbon with a disordered structure and graphitized carbon,

respectively [36]. The ratio of the intensity of the D peak to the G peak (ID/IG) is 1.243, suggesting a well-structured crystalline form of the carbon in the catalyst.

Figure 4(b) displays the hysteresis loop of paper sludge-based Co/Fe composite catalyst at room temperature. The results show that the saturation magnetization of the catalyst is 6.15 emu/g, indicating that the catalyst possesses a certain degree of magnetism. The magnetic properties of the catalyst facilitate its recovery, enhancing both the applicability and reusability of the paper mill sludge-based Co/Fe composite catalyst.
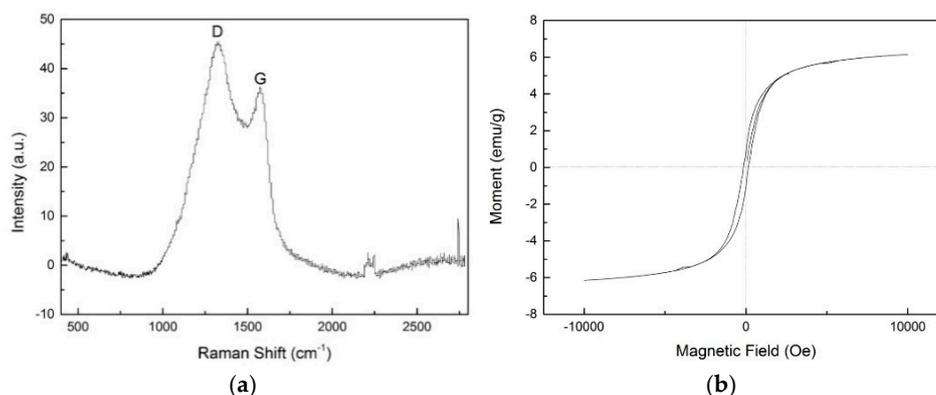

Figure 4. Raman spectra (a) and Magnetic hysteresis loops (b) of the catalyst.

The paper sludge-based Co/Fe composite catalysts prepared under optimal conditions were determined by BET, and the results of the specific surface area (S_{BET}), microporous area (S_{micro}), external surface area (including mesopore and macroporous area, S_{ext}), microporous volume (V_{micro}), total pore volume (V_t) and average pore size (D_{ap}) were illustrated in Table 1. It can be seen that most of the catalyst surface is microporous, and the presence of micropores helps to increase the surface-active sites and enhance the catalytic effect of the catalyst.

Table 1. Characterization of the porous structure of catalyst.

Surface parameters	Surface parameters
$S_{BET}(m^2/g)$	21.126
$S_{micro}(m^2/g)$	15.03
$S_{ext}(m^2/g)$	6.09
$V_{micro}(cm^3/g)$	0.0075
$V_t(cm^3/g)$	0.0572
$D_{ap}(nm)$	10.82

The SEM image of the composite catalyst was illustrated in Figure 5, which exhibited a relatively rough surface with numerous pores. Additionally, the contents of cobalt and iron in the catalyst are 6.4% and 5.8% respectively. This porous structure increases the contact area between the catalyst surface and PMS, which accelerates the reaction rate. The porous structure facilitates enhanced contact between these metal elements and PMS, improving the catalyst's performance.
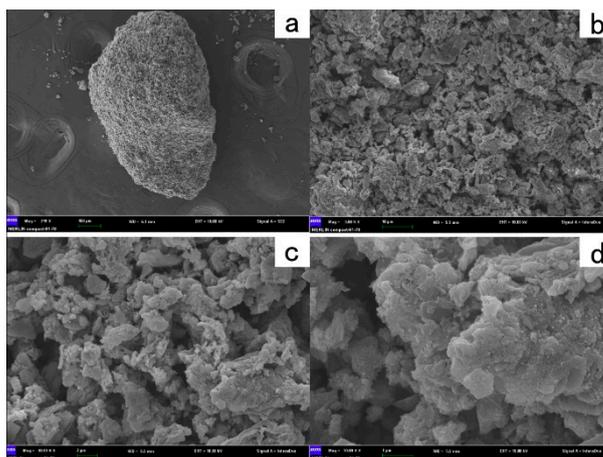
Figure 5. SEM of the Co/Fe composite catalysts.

3.3. Influence of inorganic ions on the degradation of RhB in the catalyst/PMS Fenton like reaction system

The effect of inorganic ion ($H_2PO_4^-$, NO_3^-, Cl^-, and HCO_3^-) on the degradation of RhB by PMS, catalyzed by the paper mill sludge-based Co/Fe composite catalyst, are illustrated in Figure 6. The results show that $H_2PO_4^-$ significantly hindered the degradation reaction and has an inhibitory effect on the reaction system Figure 8(a). Figure 8(b) illustrates the effect of NO_3^- on the catalytic degradation of RhB by PMS using a paper mill sludge-based Co/Fe composite catalyst. The results show that at NO_3^- concentrations of 5 mol/L and 10 mol/L, there is a noticeable promotion of the reaction system. However, when the NO_3^- concentration increases to 15 mol/L, an inhibitory effect on the reaction system becomes apparent. Figure 8(c) illustrates the effect of Cl^- on the degradation of rhodamine B by PMS activated by paper sludge-based Co/Fe composite catalyst. The results show that after adding various concentrations of Cl^-, there is almost no degradation of the dye, indicating that Cl^- has an inhibitory effect on the reaction system. Figure 8(d) shows the effect of HCO_3^- on the degradation of rhodamine B by PMS catalysed by paper sludge-based Co/Fe composite catalyst. The results indicate that the degradation reaction is significantly hindered after the addition of different concentrations of HCO_3^-.
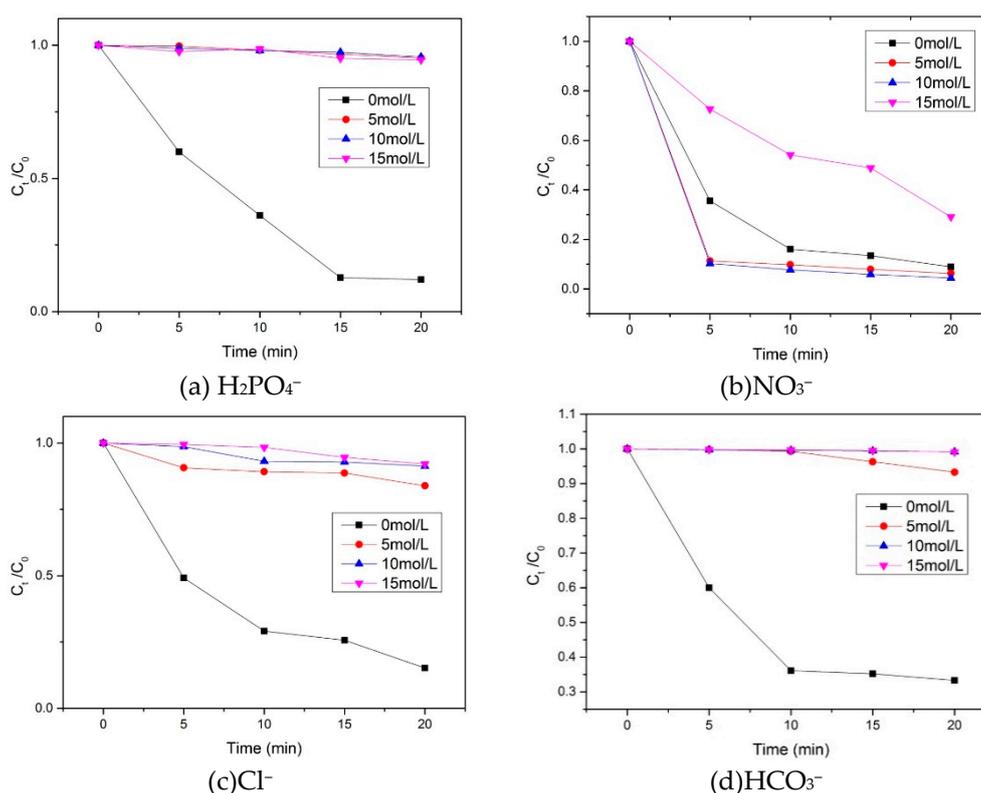

(a) $H_2PO_4^-$

(b) NO_3^-

(c) Cl^-

(d) HCO_3^-

Figure 6. Effect of different concentrations of inorganic ions $H_2PO_4^-$ (a) , NO_3^- (b), Cl^- (c), and HCO_3^-(d) on the degradation of RhB with Co/Fe-PMS system ([RhB]= 50mg/L, [PMS]=0.05mol/L, [catalyst]= 0.2g/L).

4. Discussion

The concentration of $Co(NO_3)_2$ during impregnation is crucial for the synthesis of Co-based catalysts. The concentration of $Co(NO_3)_2$ directly influences the amount of cobalt deposited on the support. The concentration can also affect the size and dispersion of cobalt particles. At an appropriate concentration, cobalt particles can be well-dispersed on the support, maximizing the surface area available for catalysis. However, too high a concentration may lead to particle agglomeration, reducing the effective surface area and catalytic activity. Given the environmental and health risks associated with metal of cobalt, it is essential to minimize its use while maximizing its catalytic effectiveness. Therefore, selecting the optimal $Co(NO_3)_2$ impregnation concentration is key to the efficient preparation of these catalysts.

The improved bimetallic composite catalytic performance is likely due to better dispersion and the structural valence of the active components, as well as the synergistic effects in the redox reaction when Co and Fe are used together. The combination of Co and Fe can lead to synergistic effects in redox reactions. Cobalt and iron can form a redox couple, facilitating the transfer of electrons between them. This enhanced electron transfer can accelerate the redox reaction and improve the catalytic performance.

The study demonstrates that Co/Fe bimetallic catalysts present significant potential for enhancing catalytic performance. This is due to the synergistic effects between the active sites, as well as the reduced amount of cobalt required when compared to using Co alone. These catalysts provide a promising approach for improving catalytic efficiency. FT-IR and XRD analyses confirmed that Fe and Co were successfully loaded onto the paper sludge carbon. The resulting material was found to be both porous and magnetic, facilitating easy recycling use.

The inhibition of $H_2PO_4^-$ ion may be due to the interaction between $SO_4^{\bullet-}$ and $H_2PO_4^-$, which produces less reactive $H_2PO_4^{\bullet}$. The inhibition of high concentration of NO_3^- may be due to the interaction between $SO_4^{\bullet-}$ and NO_3^-, which produces less reactive $NO_3^{\bullet}$. This reaction reduces the availability of $SO_4^{\bullet-}$ radicals that are necessary for degrading rhodamine B, thereby inhibiting the reaction, while the promotion at low concentrations might have led to the generation of other free radical species with relatively higher activity [37]. The inhibition of Cl^- is primarily due to the reaction where $SO_4^{\bullet-}$ oxidizes Cl^- to produce $Cl^{\bullet}$ (Eq. 2). The reactivity of $Cl^{\bullet}$ is lower than that of $SO_4^{\bullet-}$, which results in a reduction in the generation of the more effective $SO_4^{\bullet-}$ radicals, thereby inhibiting the reaction [38,39]. The inhibition of HCO_3^- is likely due to the hydrolysis of HCO_3^- producing alkaline conditions, which may alter the pH of the reaction mixture. In such alkaline environments, Fe^{3+} becomes inactive by forming $Fe(OH)_3$ colloids, and Co^{2+} is deactivated through precipitation. These changes reduce the reaction rate, thus demonstrating the inhibitory impact of HCO_3^- on the degradation process. Regarding the influence of anions on the Fenton-like reaction system in this study, $H_2PO_4^-$, Cl^-, and HCO_3^- were found to have inhibitory effects on the reaction. In contrast, low concentrations of NO_3^- promoted the reaction system, while high concentrations of NO_3^- inhibited it. This finding is very important for the practical application of paper sludge-based Co/Fe composite catalysts.

Institutional Review Board Statement: Not applicable.

Informed Consent Statement: Not applicable.

Conflicts of Interest: The authors declare no conflict of interest.

References

1. Liu, X.; Qin, H.; Xing, S.; Liu, Y.; Chu, C.; Yang, D.; Duan, X.; Mao S. Selective removal of organic pollutants in groundwater and surface water by persulfate-assisted advanced oxidation: The role of electron-donating capacity. *Environ. Sci. Technol.* 2023, *57*, 13710-13720. 10.1021/acs.est.3c04870

2. Li, X.; Shen, J.; Cao, H.; Zhang, W.; Sun, Z.; Ma, F.; Gu, Q. Molecular transformation of dissolved organic matter during persulfate-based advanced oxidation: Response of reaction pathways to structure. *Chem. Eng. J.* 2023, *474*, 146256-146265. https://doi.org/10.1016/j.cej.2023.146256

3. Jaafarzadeh, N.; Ghanbari, F.; Ahmadi, M.; Omidinasab, M. Efficient integrated processes for pulp and paper wastewater treatment and phytotoxicity reduction: Permanganate, Electro-Fenton and Co$_3$O$_4$/UV/peroxymonosulfate. *Chem. Eng. J.* 2016, *308*, 142-150. S1385894716312517

4. Qiu, F.; Pan, Y.; Wang, L.; Song, H.; Liu, X.; Fan, Y.; Zhang, S. Ultrafast degradation of organic pollutants in an Fe$_3$O$_4$-CoS$_2$-x activated persulfate catalytic system with an Fe-Co catalytic cycle involving oxygen and sulfur vacancies. *Sep. Purif. Technol.* 2024, *330*, 125139-125155. S1383586623020476.

5. Anipsitakis, G.P.; Dionysiou, D.D. Degradation of organic contaminants in water with sulfate radicals generated by the conjunction of peroxymonosulfate with cobalt. *Environ. Sci. Technol.* 2003, *37*, 4790-4797. 10.1021/es0263792.

6. Chamarro, E.; Marco, A.; Esplugas, S. Use of Fenton reagent to improve organic chemical biodegradability. *Water Res.* 2001, *35*, 1047-1051. S0043135400003420.

7. Khan, S.; He, X.; Khan, J.A.; Khan, H.M.; Boccelli, D.L.; Dionysiou, D.D. Kinetics and mechanism of sulfate radical- and hydroxyl radical-induced degradation of highly chlorinated pesticide lindane in UV/peroxymonosulfate system. *Chem. Eng. J.* 2017, *318*, 135-142. S138589471630,8075.

8. Wang, J.; Wang, S. Reactive species in advanced oxidation processes: Formation, identification and reaction mechanism. *Chem. Eng. J.* 2020, *401*, 126158-126176. S1385894720322865.

9. Anipsitakis, G.P.; Dionysiou, D.D. Radical generation by the interaction of transition metals with common oxidants. *Environ. Sci. Technol.* 2004, *38*, 3705-3712. 10.1021/es035121o.

10. Ma, Y.; Wang, H.; Lv, X.; Xiong, D.; Xie, H.; Zhang, Z. Three dimensional ordered mesoporous Co$_3$O$_4$/peroxymonosulfate triggered confined heterogeneous catalysis for rapid removal of ranitidine in aqueous solution. *Chem. Eng. J.* 2022, *443*, 136495-136507. S1385894722019908.

11. Xu, L.; Qi, L.; Sun, Y.; Gong, H.; Chen, Y.; Pei, C.; Gan, L. Mechanistic studies on peroxymonosulfate activation by g-C$_3$N$_4$ under visible light for enhanced oxidation of light-inert dimethyl phthalate. *Chinese J. Catal.* 2020, *41*, 322-332. S1872206719634479

12. Xie, X.; Xie, R.; Suo, Z.; Huang, H.; Xing, M.; Lei, D. A highly dispersed Co–Fe bimetallic catalyst to activate peroxymonosulfate for VOC degradation in a wet scrubber. *Environ. Sci.: Nano.* 2021, *8*, 2976–2987. 10.1039/D1EN00547B.

13. Zhang, W.; Zhang, S.; Chen, Z.; Zhang, Z. Cobalt-ferrite functionalized graphitic carbon nitride (CoFe$_2$O$_4$@gC$_3$N$_4$) nanoconfined catalytic membranes for efficient water purification: performance and mechanism. *J. Mater. Chem. A.* 2023, *11*, 18933-18944. 10.1039/D3TA03247G.

14. Dou, X.; Chen, D.; Hu, Y.; Feng, Y.; Dai, X. Carbonization of heavy metal impregnated sewage sludge oriented towards potential co-disposal. *J. Hazard. Mater.* 2016, *321*, 132-145. S0304389416308135.

15. Zhang, X.; Liu, L.; Zhao, X.; Li, Q.; Wu, Z.; Chen, J. Degradation of organic pollutants using a ternary heterojunction catalyst (CoS$_2$/CoCo$_2$O$_4$–MnFe$_2$O$_4$) for activating peroxymonosulfate with magnetic separation, anti-ion interference, and low ion leaching. *Environ. Sci.: Nano.* 2024, *11*, 4211-4229. 10.1039/D4EN00475B.

16. Zhang, Y.; Li, W.; Wang, T.; Zhang, X.; Yu, H.; Lu, J. Modulating electronic structure engineering of atomically dispersed cobalt catalyst in Fenton-like reaction for efficient degradation of organic pollutants. *Environ. Sci. Technol.* 2023, *57*, 4207–4217. 10.1021/acs.est.3c04712.

17. Jiang, Z; Wei, J.; Zhang, Y.; Niu, X.; Li, J.; Li, Y.; Pan, G.; Xu, M.; Cui, X.; Cui, N.; Li, J. Electron transfer mechanism mediated nitrogen-enriched biochar encapsulated cobalt nanoparticles catalyst as an effective persulfate activator for doxycycline removal. *J. Clean. Prod.* 2023, *384,* 135641-135651. https://www.sciencedirect.com/science/article/abs/pii/S0959652622052155

18. Liu, B.; Guo, W.; Wang, H.; Si Q., Zhao, Q.; Luo, H., Ren N. Activation of peroxymonosulfate by cobalt-impregnated biochar for atrazine degradation: The pivotal roles of persistent free radicals and ecotoxicity

assessment. *J. Hazard. Mater*. 2020, *398*, 122768-122779.   https://www.sciencedirect.com/science/article/abs/pii/S0304389420307573

19. Wang, Q.; Wei, W.; Gong, Y.; Yu, Q.; Li, Q.; Sun, J.; Yuan, Z. Technologies for reducing sludge production in wastewater treatment plants: State of the art. *Sci. Total Environ.* 2017, *587-588608*, 510-521. S0048969717304618.

20. Gherghel, A.; Teodosiu, C.; De Gisi, S. A review on wastewater sludge valorisation and its challenges in the context of circular economy. *J. Clean. Prod.* 2019, *228*, 244-263. https://www.sciencedirect.com/science/article/abs/pii/S0959652619313319

21. Tu, Y.; Tian, S.; Kong, L.; Xiong, Y. Co-catalytic effect of sewage sludge-derived char as the support of Fenton-like catalyst. *Chem. Eng. J.* 2012, *185-186*, 44-51. S1385894712000113.

22. Hadi, P.; Xu, M.; Ning, C.; Lin, C.S.K.; McKay, G. A critical review on preparation, characterization and utilization of sludge-derived activated carbons for wastewater treatment. *Chem. Eng. J.* 2015, *260*, 895-906. S138589471401153X.

23. Scoton, E.J.; Battistelle, R.A.G.; Bezerra, B.S.; Akutsu, J. A sewage sludge co-composting process using respirometric monitoring method in hermetic rotary reactor. J. Clean. Prod. 2016, *121*, 169-175. S0959652615004564.

24. Martin, M.J.; Serra, E.; Ros, A.; Balaguer, M.D.; Rigola, M. Carbonaceous adsorbents from sewage sludge and their application in a combined activated sludge-powdered activated carbon (AS-PAC) treatment. *Carbon*. 2004, *42*, 1389-1394. S0008622304000491

25. Wen, G.; Pan, Z.H.; Ma, J.; Liu, Z.Q.; Zhao, L.; Li, J.J. Reuse of sewage sludge as a catalyst in ozonation-efficiency for the removal of oxalic acid and the control of bromate formation. J. Hazard. Mater. 2012, 239-240, 381-388. S0304389412009272.

26. Cha, J.S.; Choi, J.C.; Ko, J.H.; Park, Y.K.; Park, S.H.; Jeong, K.E.; Kim, S.S.; Jeon, J.K. The low-temperature SCR of NO over rice straw and sewage sludge derived char. *Chem. Eng. J.* 2010, *156*, 321-327. S1385894709007190.

27. Wang, X.; Zhao, B.; Yang, X. Co-pyrolysis of microalgae and sewage sludge: Biocrude assessment and char yield prediction. *Energy Convers. Manag*. 2016, *117*, 326-334. S0196890416301364.

28. Chen, H.; Chen, D.; Liu, H. Influences of activation agent impregnated sewage sludge pyrolysis on emission characteristics of volatile combustion and De-NOx performance of activated char. Appl. Energy. 2015, *156*, 767-775. S030626191500731X.

29. Zhang, J.; Wang, Q. Sustainable mechanisms of biochar derived from brewers' spent grain and sewage sludge for ammonia–nitrogen capture. *J. Clean. Prod.*, 2016, *112*, 3927-3934. S0959652615010252.

30. Monsalvo, V.M.; Mohedano, A.F.; Rodriguez, J.J. Activated carbons from sewage sludge: Application to aqueous-phase adsorption of 4-chlorophenol. *Desalination*. 2011, *277*, 377-382. S0011916411003973.

31. Carrasco-Díaz, M.R.; Castillejos-López, E.; Cerpa-Naranjo, A.; Rojas-Cervantes, M.L. Efficient removal of paracetamol using $LaCu_{1-x}M_xO_3$ (M=Mn,Ti) perovskites as heterogeneous Fenton-like catalysts. *Chem. Eng. J.* 2016, 304, 408-418. S1385894716308610.

32. Sashkina, K.A.; Polukhin, A.V.; Labko, V.S.; Ayupov, A.B.; Lysikov, A.I.; Parkhomchuk, E.V. Fe-silicalites as heterogeneous Fenton-type catalysts for radiocobalt removal from EDTA chelates. *Appl. Catal. B: Environ.* 2016, *185*, 353-361. S0926337315303222.

33. Yuan, S.J.; Dai, X.H. Facile synthesis of sewage sludge-derived mesoporous material as an efficient and stable heterogeneous catalyst for photo-Fenton reaction. *Appl. Catal. B: Environ.* 2014, *154-155*, 252-258. S0926337314001246.

34. Yao, Y.；Cai, Y.; Wu, G.; Wei F.; Li X.; Chen H.; Wang S. Sulfate radicals induced from peroxymonosulfate by cobalt manganese oxides $(Co_{(x)}Mn_{(3-x)}O_4)$ for Fenton-Like reaction in water. *J. Hazard. Mater*. 2015, 296, 128-137. S0304389415002964.

35. Simaioforidou, A.; Papastergiou, M.; Margellou, A.; Petrakis, D.; Louloudi, M. Activated vs. pyrolytic carbon as support matrix for chemical functionalization: Efficient heterogeneous non-heme Mn(II) catalysts for alkene oxidation with H_2O_2. *J. Mol. Catal*. *A: Chem.* 2017, *426*, 516-525. S1381116916303685.

36.   Lin K. Y. A.; Chen Y. C.; Huang C. F. Magnetic carbon-supported cobalt prepared from one-step carbonization of hexacyanocobaltate as an efficient and recyclable catalyst for activating Oxone. Sep. Purif. Technol., 2016; 170: 173-182. S1383586616308747.

37.   Chen, X.Y.; Chen, J.W.; Yang, P.; Qiao, X.L. Influential Factors and Degradation Pathway of Imidacloprid by Homogeneous Co/PMS System. *Environ. Sci.* 2007, 28, 2816-2820. 18290443

38.   Ouyang, B.; Fang, H.J.; Zhu, C.Z.; Dong, W.B.; Hou H.Q. Reactions between the $SO_4^{\bullet-}$ radical and some common anions in atmospheric aqueous droplets. *J. Environ. Sci.* 2005,17, 786-788. jes17-5-16.

39.   Yu, X.Y.; Bao, Z.C.; Barker, J.R. Free radical reactions involving $Cl^{\bullet}$, $Cl_2^{-\bullet}$, and $SO_4^{\bullet-}$ in the 248 nm photolysis of aqueous solutions containing $S_2O_8^{2-}$ and Cl^-. *Chem. Inform.* 2004, *35*, 295-308. 10.1021/jp036211.